

Title page:

Characterization of microsomal CYP-dependent monooxygenases in
the rat olfactory mucosa.

Anne-Laure Minn, H el ene Pelczar, Claire Denizot, Michel Martinet, Jean-Marie
Heydel, Bernard Walther, Alain Minn, Herv e Goudonnet, and Yves Artur.

UMR 1234 Toxicologie Alimentaire, INRA-Universit e de Bourgogne, Facult e de Pharmacie,
7 boulevard Jeanne d'Arc, BP 87900, 21079 Dijon Cedex, France (A-LM, HP, J-MH, HG,
YA) ; Technologie Servier, 27 Rue Eug ene Vignat : POB 1749, 45007 Orl eans Cedex 1,
France (CD, MM, BW) ; UMR CNRS-UHP 7561, Laboratoire de Pharmacologie, Facult e de
M edecine, BP 184, 54505 Vand oeuvre-l es-Nancy, France (AM)

Running title :

CYP mRNA expression and activity in the rat olfactory mucosa.

Corresponding author:

Pr Y. Artur,

UMR 1234 Toxicologie Alimentaire, INRA-Université de Bourgogne,

Faculté de Pharmacie,

7, boulevard Jeanne d'Arc

BP 87900

21079 DIJON Cedex

Tel: +(33) 380393251

Fax: +(33) 380393218

Email : yves.artur@u-bourgogne.fr

Number of text pages: 26

Number of tables: 6

Number of figures: 3

Number of references: 44 (max 40)

Number of words in the Abstract: 253 (max 250)

Number of words in the Introduction: 718 (no more than 750)

Number of words in the Discussion: 2461 (max 1500)

Abbreviation used:

CYP, cytochrome P450 isoform; OM, olfactory mucosa; MOP, methoxsalen.

Abstract:

Nasal administration of a drug ensures therapeutic action by rapid systemic absorption and/or the entry of some molecules into the brain through different routes. Many recent studies have pointed out the presence of xenobiotic metabolizing enzymes in rat olfactory mucosa (OM). Nevertheless, very little is known about the precise identity of isoforms of CYP-dependent monooxygenases (CYP) and their metabolic function in this tissue. Therefore, we evaluated mRNA expression of 19 CYP isoforms by semi-quantitative RT-PCR and measured their microsomal activity toward six model substrates. For purposes of comparison, studies were conducted on OM and the liver. Specific activities toward phenacetin, chlorzoxazone and dextrometorphan are higher in OM than in the liver; those toward lauric acid and testosterone are similar in both tissues and that toward tolbutamide is much lower in OM. There are considerable differences between the two tissues with regard to mRNA expression of CYP isoforms. Some isoforms are expressed in OM but not in the liver (CYP1A1, 2G1, 2B21 and 4B1), whereas mRNA of others (CYP2C6, 2C11, 2D2, 3A1, 3A2 and 4A1) are present only in hepatic tissue. Although expression of CYP1A2, 2A1, 2A3, 2B2, 2D1, 2D4, 2E1, 2J4 and 3A9 is noticed in both tissues, there are a number of quantitative differences. On the whole, our results strongly suggest that CYP1A1, 1A2, 2A3, 2E1, 2G1 and 3A9 are among the main functional isoforms present in OM, at least regarding activities toward the 6 tested substrates. The implication of olfactory CYP-dependent monooxygenases in toxicology, pharmacology and physiology should be further investigated.

Introduction

Nasal administration of drugs is considered to be an interesting alternative to the oral route. It allows a systemic passage through the respiratory mucosa which avoids the first hepatic passage and gives direct access to the brain through the olfactory mucosa (OM). Rapid transport to the brain may result from a paracellular passage into the cerebrospinal fluid, and more slowly from an intracellular passage followed by axonal transport (Minn et al., 2002). Besides, the presence of drug metabolizing enzymes in olfactory tissues is well established, especially monooxygenase-dependent activities related to the cytochrome P450 (CYP) superfamily, and conjugating enzymes such as UDP-glucuronosyltransferases, glutathione-S-transferases, sulfotransferases and epoxide hydrolases (for reviews, see Thornton-Manning and Dahl, 1997; Minn et al., 2002). Altogether these enzymes form a complete system for the detoxification and elimination of xenobiotics, which may decrease the bioavailability of drugs administered by the nasal route. Conversely, several substrates may be activated to toxic metabolites by CYP activities. Indeed, CYP catalyse the formation of reactive intermediates and free radicals able both to bind and to alter DNA or proteins and to promote unsaturated lipid peroxidation and membrane destabilisation. Thus, CYP-dependent metabolism may trigger nasal toxicity or tumorigenesis.

Olfactory CYP activities and/or expression have been studied in mice, rats, rabbits, dogs and monkeys (Thornton-Manning and Dahl, 1997), animals commonly used for drug development. Recently, Zhuo et al. (2004) generated homozygous *Cyp2g1*-null mice, which do not express the specific olfactory CYP2G1. However, studies in man are scarce (Ding and Kaminsky, 2003) because of the difficulty to obtain olfactory tissue samples.

In rats, CYP-dependent activities were described about twenty years ago in both olfactory and respiratory mucosa (Hadley and Dahl, 1982). Some studies specifically concern

the formation of toxic metabolites by OM after the administration of various molecules and thus the potential role of CYP in nasal toxic events (Ding et al., 1996; Gu et al., 1998; Longo et al., 2000). Recent papers focus on the possible induction of olfactory isoforms (Genter et al. 2002; Robottom-Feirreira et al., 2003). Only a few authors report a comparison between CYP activities or expression in OM and the liver. Among them, Hadley and Dahl (1982) compared CYP-dependent activities toward para-nitroanisole, aniline, aminopyrine, and hexamethylphosphoramide in the OM and liver of rats. They observed that CYP activities in OM were of the same order of magnitude or higher than those in the liver. Several CYP present in the liver were also revealed by western blot or immunohistochemistry in OM: CYP1A1/2, CYP2B1, CYP2C, CYP2E1, CYP2J4 and CYP3A1 (Chen et al., 1992; Zhang et al., 1997; Wardlaw et al., 1998; Deshpande et al., 1999; Genter et al., 2002). CYP2A3 protein, weakly expressed in the liver, is largely expressed in olfactory tissues (Chen et al., 1992). Moreover, a specific isoform, CYP2G1, exclusively expressed in OM has been characterised by Nef et al. (1989). Published data report the detection of only four mRNA coding for CYP2A3, 2E1, 2G1 and 2J4 in rat OM, using either northern blot (Nef et al., 1989; Zhang et al., 1997; Longo et al., 2000) or, more recently, RT-PCR (Wang et al., 2002; Robottom-Feirreira et al., 2003).

Considering the major role of these enzymes in pharmacology and toxicology, and observing that data from the literature are often fragmentary, it seemed necessary to carry out a more exhaustive study of CYP activities and expression in olfactory tissues and to compare them with those in the liver, the main drug metabolizing organ. To this end, we measured in the liver and OM microsomes CYP activities toward 6 different model substrates: phenacetin, chlorzoxazone, tolbutamide, lauric acid, dextromethorphan and testosterone. These molecules are classically used in the evaluation of liver activities involving the CYP1A, 2E1, 2C, 4A, 2D and 3A isoforms, respectively. Various inhibitors were tested in order to clarify the role of

certain isoforms in the metabolism of the model substrates: ketoconazole, furafylline, α -naphthoflavone, diethyldithiocarbamate, quinine, and 5- and 8-MOP. These compounds are known to inhibit CYP3A, 1A2, 1A, 2E1, 2D, and 2A3 and 2G1, respectively. Using semi-quantitative RT-PCR, a quite suitable method for intertissue comparison studies, we determined mRNA expression of 19 CYP isoforms in the OM and liver. Considering our results and data from the literature reporting the use of recombinant enzymes, we provide original element for the identification of CYP isoforms involved in the metabolic activity of OM.

2. Materials and Methods

2.1. Chemicals

¹⁴C-labeled substrates were purchased from Amersham (Amersham Biosciences Europe, Orsay, France), except ¹⁴C-phenacetin, purchased from Sigma (Sigma Aldrich, Saint Quentin-Fallavier, France). All unlabeled substrates and reference chemicals for each metabolite were purchased from Sigma, except 6-OH-chlorzoxazone, purchased from Ultrafine Chemicals Ltd (Manchester, UK), and dextrorphan-D-tartrate from ICN Biomedicals (ICN Pharmaceuticals France SA, Orsay, France).

Enzymes and chemicals used for RT-PCR were purchased from Promega France SARL (Charbonnières-les-Bains, France), except Taq polymerase, purchased from Eurobio (Les Ulis, France).

2.2. Animals

Male Wistar rats (180-200 g) were supplied by Iffa Credo (Iffa Credo, Saint-Germain-sur-L'Arbresle, France), and housed in a room maintained at 20-22 °C with a 12 hr/12 hr

light/dark cycle. The animals received standard rodent chow and tap water *ad libitum* and were acclimatized for at least 1 week prior to experiments. The study protocol was approved by the local Animal Ethics Committee, and the research complied with the “NIH Principles of Laboratory Animal Care”.

The rats were killed by decapitation. The olfactory epithelium was carefully scraped from the nasal cavity and placed into a sterile phosphate buffer (0.05 M, pH 7.4) to remove any cartilage debris. The liver was also harvested and immersed in sterile phosphate buffer. The samples of epithelium and liver were immediately frozen in liquid nitrogen and stored at -80°C until used.

Microsomes were prepared from a pool of five livers and a pool of 40 olfactory epithelia as described by Gradinaru et al. (1999).

2.3. Measurement of CYP-dependent activities

Standard incubation mixtures (500 μl , final volume) contained microsomes (0.25-2 mg protein), 0.1 M Tris-HCl buffer, pH 7.4, 5 mM MgCl_2 and the ^{14}C -labeled substrate or dextromethorphan at the concentration specified below. The mixtures were incubated at 37°C , for 10 to 30 min, with or without inhibitors. For inhibition studies, only one experiment was performed because of the small amount of available material. All inhibitors used (ketoconazole, furafylline, α -naphthoflavone, diethyldithiocarbamate, quinine, 5- and 8-MOP) were dissolved in methanol; however, the percentage of methanol within the incubation medium was never higher than 1 % of the total volume and did not interfere with the reaction. The incubation mixture was agitated for 5 min before starting the reaction by adding NADPH (2 mM, final concentration). Reactions were terminated by the addition of methanol under agitation and cooling on ice for 10 min. After centrifugation for 10 min at 1500 g, the supernatant was collected for metabolite measurements. Product formation was

determined using Packard Liquid Chromatograph HP 1100 (Agilent Technologies France, Massy, France) coupled to on-line radiochemical detection, Packard 150 TR Flow Scintillation Analyser or fluorimetric determination with Perkin Helmer LC 240 Detector (Perkin-Elmer, Courtaboeuf, France).

For measurements of testosterone hydroxylation, microsomes were incubated with 200 μM ^{14}C -testosterone (57 mCi/mmol), and the radioactive hydroxylated metabolites were separated by a combination of isocratic and solvent gradient elution. Solvent A was methanol in water (30/70 v/v), adjusted to pH 4.5 with acetic acid; solvent B was a mixture of methanol and acetonitrile (90/10 v/v), adjusted to pH 4.45 with acetic acid; solvent C was pure methanol. The initial solvent composition was 89 % buffer A and 11 % buffer B, maintained for 10 min following injection of each sample. A gradient elution was then used for the following 40 min until a ratio of 72 % A to 28 % B was obtained. This was followed by an isocratic mode for 20 min. At 60 min, elution was done with 100 % of C for 10 min. The flow-rate was 1.5 ml/min.

The other hydroxylation activities were measured by using the following substrate concentrations: ^{14}C -chlorzoxazone (57 mCi/mmol): 1000 μM ; ^{14}C -tolbutamide (61 mCi/mmol): 50 μM ; ^{14}C -lauric acid (58 mCi/mmol): 100 μM . The determination of phenacetin *O*-deethylation was based on the measurement of acetaminophen production from 200 μM ^{14}C -phenacetin (5.7 mCi/mmol). After stopping the reactions involving the different substrates (phenacetin, chlorzoxazone, tolbutamide and lauric acid), aliquots from the supernatant were analysed by HPLC using an elution solvent gradient. Solvent D was a 0.1 % solution of trifluoroacetic acid in water, while solvent E was pure acetonitrile. Gradient elution was employed as follows: 0 to 20 min: 90 % to 63 % D, and 20 to 30 min: 63 % to 40 % D, except for lauric acid metabolites for which the gradient was: 0 to 14 min: 64 % D; 14

to 18 min: 64 % to 10 % D; 18 to 25 min: 10 % D and 25 to 30 min: 0 % D. The flow-rate was 1.0 ml/min. Radioactivity was detected using on-line radiochemical detection.

Dextromethorphan demethylation was measured using a substrate concentration of 400 μ M. The dextrorphan metabolite was separated by HPLC, using solvents D and E and the following elution process (flow-rate: 1.0 ml/min): 0 to 20 min: 80 % to 53 % D; and 20 to 25 min: 53 % to 30 % D. It was detected by fluorimetry, with an excitation wavelength of 200 nm and an emission wavelength of 305 nm, and quantified by reference to a standard concentration.

2.4. Determination of apparent kinetic parameters

We determined the apparent kinetic parameters of the biotransformation of testosterone, phenacetin, chlorzoxazone and dextromethorphan using the method of Bertrand et al. (2000). Two incubations similar to those described above were performed for each substrate with either low or high substrate concentrations and respectively low or high microsomal protein concentrations (4 or 100 μ M testosterone, and 0.05 or 0.5 mg/ml of microsomal proteins; 1 or 100 μ M phenacetin, and 0.1 or 0.5 mg/ml of microsomal proteins; 5 or 500 μ M chlorzoxazone, and 0.05 or 0.5 mg/ml of microsomal proteins; 1.5 or 150 μ M dextromethorphan, and 0.1 or 0.5 mg/ml of microsomal proteins). Aliquots of the incubation mixture were sampled at 0, 5, 15, 30, and 60 min. Residual substrate concentrations were measured at each time, and data were analysed with WinOnLine software (Pharsight Corporation, Mountain View, USA) to obtain apparent K_m and V_{max} values.

2.5. RT-PCR

Total RNA was extracted according to a microscale method, using a RNAXEL kit (Eurobio, Les Ulis, France) and RNA concentration was determined by spectrophotometry.

To avoid any contamination of the RNA by genomic DNA, a DNase treatment was performed using RNase-free DNase (RQ1; Promega, Madison, WI). Complementary DNA was synthesized from RNA samples by mixing 1 µg of total RNA, 100 pmol of random hexamer in the presence of 50 mM Tris-HCl buffer (pH 8.3); 75 mM KCl; 3 mM MgCl₂; 10 mM dithiothreitol; 200 units of Moloney Murine Leukemia Virus reverse transcriptase; 40 units of RNase inhibitor and 1 mM of each dNTP in a total volume of 20 µl. Samples were incubated at 37 °C for 60 min and then diluted to 100 µl with sterile diethylpyrocarbonate-treated water. The reverse transcriptase was inactivated by heating at 95 °C for 5 min.

Sets of primers were designed to amplify β-actin cDNA (according to Nudel et al., 1983) and the following CYP cDNA isoforms: CYP1A1; 1A2; 2A1; 2A3; 2B2; 2B21; 2C6; 2C11; 2D1; 2D2; 2D4; 2E1; 2G1; 2J4; 3A1; 3A2; 3A9; 4A1; and 4B1 (Table 1). They were synthesized by Life Technologies (Cergy Pontoise, France). A 10 µl aliquot of cDNA was used for PCR and was added to a reaction mixture containing 20 mM Tris-HCl buffer (pH 8.5), 16 mM (NH₄)₂SO₄, 150 µg/ml bovine serum albumin, 1.5 mM MgCl₂, 0.2 mM of each dNTP, 50 pmol of each primer and 2 units of Taq DNA polymerase (Eurobio, Les Ulis, France), in a total volume of 50 µl. PCR proceeded through a 30-sec denaturing step at 94 °C, a 30-sec annealing step at a specific temperature (Table 1) and a 45-sec elongation step at 72 °C in a thermal cycler (Personal-Eppendorf, Hamburg, Germany).

The specificity of each set of primers toward liver and OM cDNA was confirmed by sequencing the RT-PCR products obtained from the liver and olfactory mucosa, respectively (Genome Express, Meylan, France). PCR negative controls were performed on both liver and OM samples (without polymerase, without cDNA, or without RT) to verify the absence of external or genomic DNA contamination.

For each isoform, comparison between mRNA expression levels in OM and liver was achieved through amplification using the appropriate specific CYP set of primers and the β-

actin primers for internal standardization. Aliquots of PCR mix were sampled at 20, 25, 30 and 35 amplification cycles. The amplified products were resolved by agarose gel electrophoresis using ethidium bromide for band revelation. The bands were visualized under UV light and photographed by a computer assisted camera (Vilber Lourmat, Marne La Vallée, France).

2.6. *Other assays*

Microsomal proteins were measured by the Kit Biorad Protein Assay Dye Reagent Concentrate (Bio-Rad, Marnes-la-Coquette, France), using fraction V of bovine serum albumin as a standard.

Results

3.1. *CYP-dependent activities*

We measured the specific activities of OM and liver microsomes toward 6 model substrates (Table 2). The transformation rate of phenacetin to acetaminophen was 8 times higher in the OM than in the liver. Likewise, OM microsomes presented an activity toward chlorzoxazone 3-times higher than that of hepatic microsomes. Activity toward tolbutamide in the OM was much lower than that in the liver and was the lowest measured in this olfactory tissue. Concerning lauric acid, the enzymatic activity was similar in OM and liver microsomes. For dextromethorphan, activity measured in OM was slightly higher than in the liver. Besides, the chromatographic analysis showed that an unidentified metabolite (named x in Figure 1) was formed by both hepatic and OM microsomes, but in different amounts. In addition, OM and the liver produced two different additional metabolites (y and z, respectively) which were not identified (Figure 1). Lastly, testosterone was metabolized at

similar rates by the microsomes of both tissues (15460 pmol/min/mg of liver protein and 11650 pmol/min/mg of OM protein). However, the hydroxy-metabolites formed in the two tissues were different (Figure 2). 15α -, 15β -, 2β -OH-testosterone, androstenedione and one unidentified metabolite were the five main products formed by OM microsomes, while 16α -, 2α -, 6β -OH-testosterone and androstenedione were the major metabolites produced by liver microsomes.

3.2. Inhibition

We tested the effects of inhibitors on OM activities toward the 4 substrates extensively metabolized by this tissue: phenacetin, chlorzoxazone, dextromethorphan and testosterone. Five inhibitors (ketoconazole, furafylline, α -naphthoflavone, diethyldithiocarbamate and quinine) were tested toward only one determined activity because of their high selectivity; the 2 others (5- and 8-MOP), less selective (see discussion), were tested toward the 4 activities (Table 3). Ketoconazole inhibited only 10 % of the activity toward testosterone whereas 5- and 8-MOP were more efficient (80 % of inhibition). For phenacetin metabolism, almost total inhibition (94%) was obtained with α -naphthoflavone. The activity toward this substrate was decreased by 50 % in the presence of furafylline, and total inhibition was obtained with 5- and 8-MOP. Addition of diethyldithiocarbamate to the incubation mixture decreased chlorzoxazone hydroxylation by 50 %, whereas 5- and 8-MOP at the highest concentration gave 90 % inhibition. The highest concentration of quinine decreased dextromethorphan metabolism by only 23 %, whereas 5- and 8-MOP totally inhibited it.

3.3. Michaelis-Menten apparent kinetic parameters

Table 4 presents apparent kinetic parameters and the efficiency of the enzyme for the 4 most intensively metabolized substrates in the OM. Determination of apparent K_m highlighted

the fact that affinities of OM microsomes toward phenacetin and chlorzoxazone were about 10 times higher than those of liver microsomes, while V_{\max} confirmed the high activity of OM toward these substrates in comparison to the liver. For dextromethorphan and testosterone, K_m and V_{\max} values were very similar in both tissues. Determination of the ratio V_{\max}/K_m suggests that the two tissues have similar metabolic capacity for testosterone and dextromethorphan and that OM metabolism is more efficient toward phenacetin and chlorzoxazone than is liver metabolism.

3.4. mRNA expression

Semi quantitative RT-PCR analysis, according to the number of amplification cycles, allowed us to compare expression levels of mRNA coding for a specific CYP isoform in liver and OM. The 2 tissues presented notable differences concerning mRNA expression of the 19 tested isoforms (Figure 3). Messenger RNA of CYP2C6, 2C11, 2D2, 3A1, 3A2 and 4A1 were not detected in OM. In contrast, those of CYP1A1, 2A3, 2B21, 2G1 and 4B1 seemed to be expressed only in OM. Messenger RNA expression of CYP1A2 and 2E1 appeared to be similar in both tissues. Finally, mRNA of CYP2A1, 2D1 and 2D4 were more strongly expressed in the liver, whereas those of CYP2B2, 2J4 and 3A9 were more strongly expressed in the OM.

Discussion

Previous studies on toxic metabolite formation have pointed out the high metabolic capacity of OM. Eriksson and Brittebo (1995) demonstrated that the CYP specific activity of OM microsomes toward dichlobenil is greater than that measured in the liver. Besides, studying the nasal toxicity of 2,6-dichlorobenzonitrile, Ding et al. (1996) observed the

formation by OM of a metabolite, dihydroxy-monochlorobenzonitrile, which was not detected after hepatic metabolism of this substrate. These examples demonstrate that metabolic differences between OM and liver do exist, suggesting qualitative and/or quantitative differences in the enzymes expressed in these tissues. Our results based on the metabolism of 6 model substrates highlight significant qualitative differences between testosterone and dextromethorphan metabolites produced by OM microsomes and those produced by liver microsomes. For chlorzoxazone and phenacetin, the measured apparent K_m also suggest a difference between the two tissues in the enzymes metabolizing these substrates. Lastly, our data demonstrate that tolbutamide is significantly metabolized only by liver microsomes.

Concerning the metabolism of our six model substrates, the only comparable data in the literature concern a rabbit model. The specific activity toward phenacetin measured by Ding and Coon (1990) in rabbit OM microsomes was 5 to 10 times higher than that in liver microsomes. This ratio is similar to what we report here in the rat (8 times higher). The specific activity of rabbit OM microsomes toward lauric acid was also measured by Laethem et al. (1992), but without comparison with hepatic microsomal activity. We found similar specific activities in both rat liver and OM microsomes toward this substrate, which were very close to that obtained by the above authors in rabbit OM.

In OM, we detected the mRNA coding for CYP1A1, 1A2, 2A3, 2E1, 2G1, 2J4 and 4B, whose expression had already been described by others at the protein level (Chen et al., 1992; Zhang et al., 1997; Wardlaw et al., 1998; Deshpande et al., 1999; Genter et al., 2002) or at the mRNA level (Nef et al., 1989; Zhang et al., 1997; Longo et al., 2000; Wang et al., 2002; Robottom-Feirreira et al., 2003). In addition, we identified for the first time the mRNA coding for CYP2A1, 2B2, 2B21, 2D1, 2D4 and 3A9. Antibodies raised against CYP2A (Su et al., 1996) or CYP2B (Wardlaw et al., 1998) have been used in OM but their lack of

specificity precluded accurate CYP identification. Even after a 35-cycle amplification, we did not observe any expression of mRNA coding for CYP2C6, 2C11, 2D2, 3A1, 3A2, and 4A1 in OM, although Western blot experiments showed that CYP2C11 and 3A2 proteins were present in very low quantities in OM (Genter et al., 2002; Deshpande et al., 1999). The conflicting results concerning CYP3A may be explained by the observations of Aiba et al. (2003): their work demonstrated the existence of an immunological cross-reaction between CYP3A2 and CYP3A9; the mRNA of the latter was clearly detected in OM in the present study. Besides, the absence of the expression of CYP2C6, 2D2, 3A1 and 4A1 in OM has not been documented until now. Lastly, among the 19 CYP isoforms we studied, the expression of six isoforms (2B21, 2D1, 2D2, 2D4, 3A9, 4A1) has never been examined in OM by immunoblotting. Antibodies are commercially available only for CYP2D and 4A, but we decided not to use these since we did not detect any significant mRNA expression of these isoforms in OM.

In order to evaluate the metabolic capacities of the CYP isoforms located in OM, we hypothesize that mRNA expression of CYP in this tissue correlates to their protein expression. Although this hypothesis may appear highly speculative, it is perfectly validated by published data for 4 CYP isoforms: CYP2A3, 2E1, 2G1 and 2J4 (Nef et al., 1989; Chen et al., 1992; Zhang et al., 1997; Wang et al., 2002; Robottom-Feirreira et al., 2003). Moreover, in OM we detected the mRNA corresponding to all CYP isoforms whose protein expression had been found by others except for CYP2C11. In addition, the recent characterization of rat recombinant CYP activities gave us reference data concerning their substrate specificities (Table 5) and their individual sensitivity to different inhibitors (Table 6).

It has been established that phenacetin is mainly metabolized by CYP1A1, 1A2 and 2C6. Other CYP, such as CYP2A2, 2C11, 2C13, 2E1, 3A1 and 3A2 can metabolize this substrate to a lesser degree, whereas CYP2A1 and 2B1 do not (Table 5). Using RT-PCR, we showed that CYP1A2 is expressed in a similar way in both OM and the liver. CYP1A1 is constitutively expressed in OM, whereas it is known to appear only after induction in the liver. CYP2C6 expression in OM remained undetectable after 35 cycles. Among the other CYP mentioned above, only CYP2E1 was expressed in OM, but in amounts similar to those in the liver. Therefore, the high activity displayed by OM toward phenacetin must involve other isoforms. Moreover, this activity was decreased by 50% in the presence of furafylline, an inhibitor of CYP1A2 and, to a lesser extent of CYP2C6 (Table 6). This inhibition confirmed the involvement of CYP1A2 in phenacetin metabolism in OM but did not exclude the implication of other CYP. Alpha-naphthoflavone, which is an inhibitor of CYP1A (Tassaneeyakul et al., 1993), strongly decreased activity toward phenacetin, but again, its specificity toward other CYP is not known. According to the literature, 5- and 8-MOP are considered as CYP2G1 and 2A3 inhibitors (Gu et al., 1998), but are also efficient on CYP1A, 2B1, 2C6 and 2C11 activities (Tassaneeyakul et al., 1993; Table 6). These compounds completely inhibited phenacetin metabolism in our OM incubations. Altogether these data strongly suggest the involvement of CYP1A2 and 2E1, but also of CYP1A1, 2G1 and 2A3 in phenacetin metabolism in OM. This hypothesis is greatly supported by our results, which show a substantial expression of CYP2G1 and 2A3 mRNA in this tissue. Nevertheless, we cannot exclude the possibility that other CYP are involved in this activity, for instance CYP3A9, which is more strongly expressed in OM than in the liver. However, there are no data available concerning the possible activity of this isoform toward phenacetin.

Data from the literature indicate that chlorzoxazone is a preferential substrate of CYP2E1, but it can also be metabolized by CYP1A1, CYP1A2, CYP2C11, CYP3A1, 3A2

and 3A9. Conversely, CYP2A1, 2A2, 2B1, 2C6, 2C13, 2D1 and 2D2 do not transform chlorzoxazone (Table 5). Comparison between OM and the liver in the relative expression levels of CYP2E1, 1A1, 1A2 and 3A9, and the absence of expression of CYP2C11, 3A1 and 3A2 in OM, has been discussed above. The specific activity toward chlorzoxazone is much higher in OM than in the liver. All these data are consistent with the involvement of CYP2E1, 1A and 3A9 in OM metabolic activity toward this substrate. However, other CYP may also be involved in this activity, as suggested by the use of diethyldithiocarbamate. This compound, which is known to act on hepatic CYP2E1 (Brady et al., 1991), inhibits chlorzoxazone hydroxylation by only 50% in OM; its specificity toward other CYP isoforms is not known. According to the literature, 5- and 8-MOP moderately inhibit CYP2E1 (Table 6). Even at high concentrations, these molecules did not totally inhibit the activity toward chlorzoxazone in OM. Thus, the inhibition we observed is consistent with the possible involvement of CYP2G1 and 2A3 in addition to that of CYP1A1, 1A2, 2E1 and 3A9 isoforms in OM metabolism of chlorzoxazone.

Because we have suggested that the same isoforms were responsible for the metabolism of phenacetin and chlorzoxazone in OM, we tested the effect of chlorzoxazone on the kinetics of the biotransformation of phenacetin and vice versa by incubating both substrates in the presence of OM and liver microsomes. A strong, competitive-type inhibition (80%) was observed with OM microsomes, whereas inhibition was less than 10% with those of the liver (data not shown). On the whole, our results strongly suggest that CYP1A1, 1A2, 2A3, 2E1, 2G1 and 3A9 metabolize phenacetin and chlorzoxazone in OM, whereas certain CYP are more specifically involved in the liver (mainly, CYP1A2 for phenacetin and CYP2E1 for chlorzoxazone).

The CYP2C family (2C6 or 2C11) is responsible for the hepatic metabolism of tolbutamide in rats (Azuma et al., 1999; Matsunaga et al., 2001). We found much weaker

tolbutamide hydroxylation activity in OM microsomes than in hepatic microsomes; among the tested substrates, tolbutamide was the least metabolized molecule in OM. This difference in the activities displayed by the two tissues probably results from the absence of detectable CYP2C11 and 2C6 expression in OM, whereas their mRNA are significantly expressed in the liver.

CYP2D2 is known to be the main CYP isoform involved in dextromethorphan metabolism. Most other tested recombinant CYP, i.e. CYP1A2, 2A1, 2A2, 2B1, 2C6, 2C11 and 2E1, do not display any affinity toward this substrate, or very weakly participate in its metabolism (CYP2C13, 2D1, 3A1 and 3A2) (Table 5). We showed that the hepatic isoforms belonging to the CYP2D family were either weakly (2D1 and 2D4) or not at all (CYP2D2) expressed in OM. Similarly, we did not find either CYP3A1 or 3A2 expression in OM. However, we did observe dextromethorphan metabolism of the same order of magnitude in OM and the liver. In our assays, quinine decreased dextromethorphan metabolism by 23%. This molecule inhibited CYP2D2, and to a lesser extent CYP2C6 and 2C11 (Table 6), but these isoforms were not expressed in OM. Unfortunately, there are no available data concerning quinine inhibition capacity toward other recombinant CYP. Finally, we showed that 5- and 8-MOP totally inhibited OM activity toward dextromethorphan. Previous reports mentioned above and our present data thus suggest that CYP2G1, 2A3 and 1A1 may be involved in dextromethorphan metabolism in OM. Concerning this substrate, we also pointed out quantitative and qualitative differences in the metabolites formed by OM and liver microsomes. Indeed, one of the metabolites (x) from dextromethorphan is produced in a greater quantity with OM microsomes than with liver microsomes. This metabolite has a retention time similar to that of 3-hydroxymorphinan, a product resulting from CYP3A-dependent metabolism of dextromethorphan (Motassim et al., 1987). Both CYP3A1 and 3A2 are not expressed in OM, but CYP3A9 is much more strongly expressed in this tissue than in the

liver. The involvement of CYP3A9 in dextromethorphan metabolism is thus possible but remains to be demonstrated.

CYP4A1 and to a lesser extent CYP4A2 and 4A3, are mainly involved in ω -hydroxylation of lauric acid (Table 5). This substrate can also undergo ω -1 hydroxylation, preferentially carried out by CYP2E1 (Clarke et al., 1994). In the present study, CYP4A1 mRNA was only found in the liver. Conversely, CYP2E1 mRNA is significantly expressed in OM, and the presence of the corresponding isoform could explain the lauric acid ω -1 hydroxylation we also observed in this tissue (data not shown). CYP4B1 can also metabolize lauric acid to ω -1- and ω -OH derivatives in the rabbit (Muerhoff et al., 1989). It is expressed in rat lung, but not in the liver (Gasser and Philpot, 1989). As its mRNA is expressed in OM, CYP4B1 could be mainly responsible for ω -hydroxylation of lauric acid in this tissue, and also for ω -1 hydroxylation in association with CYP2E1. There is no data available concerning the involvement of other CYP isoforms in lauric acid hydroxylation.

Testosterone biotransformation in the liver involves various CYP, including CYP3A and 2C, and leads to the formation of numerous metabolites (Table 5). However, the profile of metabolites obtained with our OM microsomes was very different from that obtained with liver microsomes. We observed the formation of the following metabolites by OM: 2 β -; 15 α -; and 15 β -OH-testosterone. It is well established that these metabolites can be produced from testosterone by CYP isoforms other than hepatic isoforms, such as CYP2A3 (Table 5), which is strongly expressed in OM. The liver and OM only produce two common metabolites, 6 β -OH-testosterone and androstenedione. CYP2A3 cannot form these metabolites, whereas CYP3A1, 3A2 and 2C11 can produce them (Table 5). We were unable to detect expression of the three last isoforms in OM. In contrast, CYP3A9, whose mRNA is expressed in OM, is known to metabolize testosterone, producing 2 β - and 6 β -OH derivatives (Table 5). Androstenedione, formed in smaller quantities by OM microsomes than by those of the liver,

can be produced by CYP2B, whose expression was also noticed in OM. We showed that ketoconazole weakly decreased testosterone metabolism in OM. This compound inhibited CYP3A1 and 3A2 (Table 6), which are not expressed in OM, but its action on CYP3A9 is not known. In contrast, 5- and 8-MOP efficiently inhibited OM activity toward this substrate. This inhibition might concern CYP2A3, 2B and possibly CYP2G1; the mRNA of all three are present in this tissue. Finally, the possible role of CYP2J4 in testosterone metabolism appears very limited (Zhang et al., 1997). Altogether, our data are consistent with the possible implication of CYP2G1, 2A3, 2B and 3A9 isoforms in OM metabolism of testosterone.

We noticed substantial mRNA expression of CYP2B21 in OM. The presence of this mRNA had only been found in the oesophagus and not in the liver by Brookman-Amisshah et al. (2001). However, no data are available concerning activities of the corresponding enzyme toward our model substrates. Its metabolic role in OM thus requires further investigation.

In the present work, we studied mRNA expression of a large number of CYP-dependent monooxygenases in rat OM and we measured the activity displayed by this tissue toward a series of substrates of these monooxygenases. A comparison of our experimental data with those from other related works, especially those concerning the catalytic activity of recombinant isoforms, strongly suggests that CYP1A1, 1A2, 2A3, 2E1, 2G1 and 3A9 are among the main functional CYP in OM, at least concerning activities toward the 6 tested substrates. The isoforms expressed in this tissue constitute an enzymatic CYP-dependent system, which is very different from the hepatic one.

Considering the role of CYP-dependent monooxygenases in the toxification of many xenobiotics, the differences we noticed in mRNA expression and in measured activities toward different substrates may contribute to tissue-specific toxicity events. And yet, these monooxygenases participate in the detoxification of numerous molecules, and their presence in OM could protect the brain especially from toxic substances by decreasing the direct nose-brain passage. Furthermore, these proteins frequently display strong enzymatic activities in OM, and in some cases (phenacetin and chlorzoxazone), the activities are significantly stronger than those measured in the liver. Even if the hepatic tissue mass is considerably greater than that of olfactory tissue, the possible role of olfactory metabolism in drug bioavailability should be considered, particularly for nasally-administered molecules. Besides, Nef et al. (1989) and Ding et al. (1991) suggested that CYP2G1 could be involved in the olfaction process, especially in olfactory signal termination. The functional role in olfaction of the other CYP isoforms found to be strongly expressed and active in olfactory tissue in this study needs to be further considered.

Acknowledgments

We gratefully acknowledge the technical assistance of Catherine Potin and also thank Nathalie Hanet for critical review of the manuscript.

References

Aiba T, Takehara Y, Okuno M and Hashimoto Y (2003) Poor correlation between intestinal and hepatic metabolic rates of CYP3A4 substrates in rats. *Pharm. Research* **20**:745-748.

Azuma R, Komuro M, Black SR and Mathews JM (1999) The effect of repeat administration of GTS-21 on mixed-function oxidase activities in rat. *Toxicol Lett* **110**:137-144.

Bertrand M, Jackson P and Walther B (2000) Rapid assessment of drug metabolism in the drug discovery process. *Eur J Pharm Sci* **11**:S61-72.

Brady JF, Xiao F, Wang MH, Li Y, Ning SM, Gapac JM and Yang CS (1991) Effects of disulfiram on hepatic P450IIE1, other microsomal enzymes, and hepatotoxicity in rats. *Toxicol Appl Pharmacol* **108**:366-373.

Brookman-Amissah N, Mackay AG and Swann PF (2001) Isolation and sequencing of the cDNA of a novel cytochrome P450 from rat oesophagus. *Carcinogenesis* **22**:155-160.

Chen Y, Getchell ML, Ding X and Getchell TV (1992) Immunolocalization of two cytochrome P450 isozymes in rat nasal chemosensory tissue. *Neuroreport* **3**:749-752.

Clarke SE, Baldwin SJ, Bloomer JC, Ayrton AD, Sozio RS and Chenery RJ (1994) Lauric acid as a model substrate for the simultaneous determination of cytochrome P450 2E1 and 4A in hepatic microsomes. *Chem Res Toxicol* **7**:836-842.

Deshpande VS, MB Genter, Jung C and Desai PB (1999) Characterization of lidocaine metabolism by rat nasal microsomes: implications for nasal drug delivery. *Eur J Drug Metab Pharmacokinet* **24**:177-182.

Ding XX and MJ Coon (1990) Immunochemical characterization of multiple forms of cytochrome P-450 in rabbit nasal microsomes and evidence for tissue-specific expression of P-450s NMa and NMb. *Mol Pharmacol* **37**:489-496.

Ding XX, Porter TD, Peng HM and Coon MJ (1991) cDNA and derived amino acid sequence of rabbit nasal cytochrome P450NMb (P450IIG1), a unique isozyme possibly involved in olfaction. *Arch Biochem Biophys* **285**:120-125.

Ding X, Spink DC, Bhama JK, Sheng JJ, Vaz AD and Coon MJ (1996) Metabolic activation of 2,6-dichlorobenzonitrile, an olfactory-specific toxicant, by rat, rabbit, and human cytochromes P450. *Mol Pharmacol* **49**:1113-1121.

Ding X and Kaminsky LS (2003) Human extrahepatic cytochromes P450: function in xenobiotic metabolism and tissue-selective chemical toxicity in the respiratory and gastrointestinal tracts. *Annu Rev Pharmacol Toxicol* **43**:149-173.

Dutton DR, McMillen SK, Sonderfan AJ, Thomas PE and Parkinson A (1987) Studies on the rate-determining factor in testosterone hydroxylation by rat liver microsomal cytochrome P-450: evidence against cytochrome P-450 isozyme:isozyme interactions. *Arch Biochem Biophys* **255**:316-328.

Eriksson C and Brittebo EB (1995) Metabolic activation of the olfactory toxicant, dichlobenil, in rat olfactory microsomes: comparative studies with p-nitrophenol. *Chem Biol Interact* **94**:183-196.

Gasser R and Philpot RM (1989) Primary structures of cytochrome P-450 isozyme 5 from rabbit and rat and regulation of species-dependent expression and induction in lung and liver: identification of cytochrome P-450 gene subfamily IVB. *Mol Pharmacol* **35**:617-625.

Genter MB, Apparaju S and Desai PB (2002) Induction of olfactory mucosal and liver metabolism of lidocaine by 2,3,7,8-tetrachlorodibenzo-p-dioxin. *J Biochem Mol Toxicol* **16**:128-134.

Gradinaru D, Suleman FG, Leclerc S, Heydel JM, Grillasca JP, Magdalou J and Minn A (1999) UDP-glucuronosyltransferase in the rat olfactory bulb: identification of the UGT1A6 isoform and age-related changes in 1-naphthol glucuronidation. *Neurochem Res* **24**:995-1000.

Gu J, Zhang QY, Genter MB, Lipinkas TW, Negishi M, Nebert DW and Ding X (1998) Purification and characterization of heterologously expressed mouse CYP2A5 and CYP2G1: role in metabolic activation of acetaminophen and 2,6-dichlorobenzonitrile in mouse olfactory mucosal microsomes. *J Pharmacol Exp Ther* **285**:1287-1295.

Hadley WM and Dahl AR (1982) Cytochrome P-450 dependent monooxygenase activity in rat nasal epithelial membranes. *Toxicol Lett* **10**:417-422.

Halvorson M, Greenway D, Eberhart D, Fitzgerald K and Parkinson A (1990) Reconstitution of testosterone oxidation by purified rat cytochrome P450p (III_{A1}). *Arch Biochem Biophys* **277**:166-180.

Kobayashi K, Urashima K, Shimada N and Chiba K (2002) Substrate specificity for rat cytochrome P450 (CYP) isoforms: screening with cDNA-expressed systems of the rat. *Biochem Pharmacol* **63**:889-896.

Kobayashi K, Urashima K, Shimada N and Chiba K (2003) Selectivities of human cytochrome P450 inhibitors toward rat P450 isoforms: study with cDNA-expressed systems of the rat. *Drug Metab Dispos* **31**:833-836.

Koenigs LL and Trager WF (1998) Mechanism-based inactivation of cytochrome P450 2B1 by 8-methoxypsoralen and several other furanocoumarins. *Biochemistry* **37**: 13184-13193.

Laethem RM, Laethem CL, Ding X and Koop DR (1992) P-450-dependent arachidonic acid metabolism in rabbit olfactory microsomes. *J Pharmacol Exp Ther* **262**:433-438.

Liu C, Zhuo X, Gonzalez FJ and Ding X (1996) Baculovirus-mediated expression and characterization of rat CYP2A3 and human CYP2a6: role in metabolic activation of nasal toxicants. *Mol Pharmacol* **50**:781-788.

Longo V, Ingelman-Sundberg M, Amato G, Salvetti A and Gervasi PG (2000) Effect of starvation and chlormethiazole on cytochrome P450s of rat nasal mucosa. *Biochem Pharmacol* **59**:1425-1432.

Matsunaga N, Nishijima T, Hattori K, Iizasa H, Yamamoto K, Kizu J, Takanaka A, Morikawa A and Nakashima E (2001) Application of the PKCYP-test to predict the amount of in vivo CYP2C11 using tolbutamide as a probe. *Biol Pharm Bull* **24**:1305-1310.

Minn A, Leclerc S, Heydel JM, Minn AL, Denizot C, Cattarelli M, Netter P, Gradinaru D (2002) Drug transport into the mammalian brain: the nasal pathway and its specific metabolic barrier. *J Drug Target* **10**:285-296.

Motassim N, Decolin D, Le Dinh T, Nicolas A and Siest G (1987) Direct determination of dextromethorphan and its three metabolites in urine by high-performance liquid chromatography using a precolumn switching system for sample clean-up. *J Chromatogr* **422**:340-345.

Muerhoff AS, Williams DE, Reich NO, CaJacob CA, Ortiz de Montellano PR and Masters BS (1989) Prostaglandin and fatty acid omega- and (omega-1)-oxidation in rabbit lung. Acetylenic fatty acid mechanism-based inactivators as specific inhibitors. *J Biol Chem* **264**:749-756.

Nef P, Heldman J, Lazard D, Margalit T, Jaye M, Hanukoglu I and Lancet D (1989) Olfactory-specific cytochrome P-450. cDNA cloning of a novel neuroepithelial enzyme possibly involved in chemoreception. *J Biol Chem* **264**:6780-6785.

Nguyen X, Wang MH, Reddy KM, Falck JR and Schwartzman ML (1999) Kinetic profile of the rat CYP4A isoforms: arachidonic acid metabolism and isoform-specific inhibitors. *Am J Physiol* **276**: R1691-1700.

Nudel U, Zakut R, Shani M, Neuman S, Levy Z and Yaffe D (1983) The nucleotide sequence of the rat cytoplasmic beta-actin gene. *Nucleic Acids Res* **11**:1759-1771.

Robottom-Ferreira AB, Aquino SR, Queiroga R, Albano RM and Ribeiro Pinto LF (2003) Expression of CYP2A3 mRNA and its regulation by 3-methylcholanthrene, pyrazole, and -ionone in rat tissues. *Braz J Med Biol Res* **36**:839-844.

Rowlands JC, Wang H, Hakkak R, Ronis MJ, Strobel HW and Badger TM (2000) Chronic intragastric infusion of ethanol-containing diets induces CYP3A9 while decreasing CYP3A2 in male rats. *J Pharmacol Exp Ther* **295**:747-52.

Su T, Sheng JJ, Lipinkas TW and Ding X (1996) Expression of CYP2A genes in rodent and human nasal mucosa. *Drug Metab Dispos* **24**:884-890.

Tassaneeyakul W, Birkett DJ, Veronese ME, McManus ME, Tukey RH, Quattrochi LC, Gelboin HV and Miners JO (1993) Specificity of substrate and inhibitor probes for human cytochromes P450 1A1 and 1A2. *J Pharmacol Exp Ther* **265**:401-407.

Thornton-Manning JR and Dahl AR (1997) Metabolic capacity of nasal tissue interspecies comparisons of xenobiotic-metabolizing enzymes. *Mutat Res*. **380**:43-59.

Wang H, Napoli KL and Strobel HW (2000) Cytochrome P450 3A9 catalyzes the metabolism of progesterone and other steroid hormones. *Mol Cell Biochem* **213**:127-135.

Wang H, Chanas B and Ghanayem BI (2002) Effect of methacrylonitrile on cytochrome P-450 2E1 (CYP2E1) expression in male F344 rats. *J Toxicol Environ Health A* **65**:523-537.

Wardlaw SA, Nikula KJ, Kracko DA, Finch GL, Thornton-Manning JR and Dahl AR (1998) Effect of cigarette smoke on CYP1A1, CYP1A2 and CYP2B1/2 of nasal mucosae in F344 rats. *Carcinogenesis* **19**:655-662.

Warrington JS, Court MH, Greenblatt DJ and von Moltke LL (2004) Phenacetin and chlorzoxazone biotransformation in aging male Fischer 344 rats. *J Pharm Pharmacol* **56**:819-825.

Waxman DJ, Lapenson DP, Park SS, Attisano C and Gelboin HV (1987) Monoclonal antibodies inhibitory to rat hepatic cytochromes P-450: P-450 form specificities and use as probes for cytochrome P-450-dependent steroid hydroxylations. *Mol Pharmacol* **32**:615-624.

Zhang QY, Ding X and Kaminsky LS (1997) CDNA cloning, heterologous expression, and characterization of rat intestinal CYP2J4. *Arch Biochem Biophys* **15**:270-278.

Zhuo X, Gu J, Behr MJ, Swiatek PJ, Cui H, Zhang QY, Xie Y, Collins DN and Ding X (2004) Targeted disruption of the olfactory mucosa-specific Cyp2g1 gene: impact on acetaminophen toxicity in the lateral nasal gland, and tissue-selective effects on Cyp2a5 expression. *J Pharmacol Exp Ther* **308**:719-28.

Footnotes

The authors would warmly thank the “Conseil Régional de Bourgogne, Dijon” and “Technologie Servier, Orléans” for financial support.

Figure 1: Dextromethorphan metabolism

Typical liquid chromatography profiles obtained after a 15-min incubation period at 37 °C of the reaction mixture. Mix contained 0.1 M Tris-HCl buffer; pH 7.4; 5 mM MgCl₂; dextromethorphan (400 μM) and 0.25 mg/ml of microsomal proteins from rat olfactory mucosa (A) or liver (B). Reaction was initiated by addition of NADPH to a final concentration of 2 mM. Metabolites were detected by fluorimetry, with an excitation wavelength of 200 nm and an emission wavelength of 305 nm.

D: dextromethorphan; d: dextrorphan; x, y and z: unidentified metabolites of dextromethorphan.

Figure 2: Testosterone metabolism

Typical liquid chromatography profiles obtained after a 10-min incubation period at 37 °C of the reaction mixture. Mix contained 0.1 M Tris-HCl buffer; pH 7.4; 5 mM MgCl₂; ¹⁴C-testosterone 200 μM (57 mCi/mmol) and 0.25 mg/ml of microsomal proteins from rat olfactory mucosa (A) or liver (B). Reaction was initiated by addition of NADPH to a final concentration of 2 mM. Radioactivity was detected using on-line radiochemical detection.

t: testosterone; a: androstenedione; x: unidentified metabolite; 2α, 2β, 6β, 15α, 15β, 16α: hydroxylated metabolites of testosterone.

Figure 3: Messenger RNA expression of various CYP isoforms in rat OM and liver, according to the number of amplification cycles. Aliquots of PCR mix were sampled at 20, 25, 30 and 35 amplification cycles. The amplified products were resolved by agarose gel electrophoresis and ethidium bromide was used for band revelation under UV light. For each isoform, the same electrophoretic gel was used for the detection of amplicons from both tissues. Five independent assays were performed, of which this picture is representative.

Table 1

Specifications for mRNA determination of rat CYP isoforms. Sequences concerning the internal standard, β -actin, are from Nudel et al. (1983). Each set of primer was carefully designed to avoid primer dimerisation and to ensure specificity of amplification. Specific annealing temperatures were verified by the use of a gradient thermal cyclers.

Isoforms	GenBank Accession number	Primer sens (5' → 3')	Primer antisens (5' → 3')	Annealing temperature (°C)	Size of PCR product (bp)
CYP1A1	NM_012540	atgccaatgtccagctctc	ggaactcgtttggatcacc	58	393
CYP1A2	NM_012541	catccctcaggagaagattg	tgaactccagctgatgca	57	542
CYP2A1	NM_012692	cttcgactatgaggacacgga	ccagcaaagaagaggcttagtg	60	333
CYP2A3	NM_012542	cgggctttcaaaggcta	cgtggaccttagcctcaatat	58	662
CYP2B2	M34452	gactttgggatgggaaagag	agagccaatcacctgatcaa	58	627
CYP2B21	NM_198733	tggacagaagaggtctctca	gagcaggtgcagaaactggt	60	461
CYP2D1	NM_153313	tggacctcagtaacatgcca	gatgcaaggatcacaccttg	57	225
CYP2D2	NM_012730	ggtggactttgagaacatgc	ttgcatctctgctagggaagg	58	699
CYP2D4	AB008424	ggctttcaaaagctgagatgtc	cctgggatgtgtagggagcat	60	536
CYP2C6	XM_215255	cgggaagtcatacgcacattagc	gcagagaggcaaatcattg	61	759
CYP2C11	J02657	aggacatggccaateaa	gggtaaacactagactgcgga	60	708
CYP2E1	NM_031543	gtctgaggctcatgagtttg	tctggaaactcatggctg	56	628
CYP2G1	XM_341809	cagtattttccaggaagac	atctttgaggactgagcca	55	524
CYP2J4	NM_023025	ctcgtggaagccataagagag	tgggtagaggccatgtaga	60	495
CYP3A1	NM_173144	aattc gatgtggatgcat	cggatagggtgtatgagattc	60	702
CYP3A2	NM_153312	gtcaaacgcctgtgtttgcc	atcagggtgagtggccagga	56	754
CYP3A9	NM_147206	cagccacctatttgagtg	taactgactggccacaatctc	61	347
CYP4A1	NM_175837	agctcactaattccgttg	gagctttttgtgcaggacact	59	542
CYP4B1	NM_016999	tttggatcacccttgagat	agggccatgcagtagagaaa	60	836
β -actin	NM_031144	tgcagaaggagattactgcc	cgcagctcagtaacagtcc	60	220

Table 2

CYP-dependent specific activities measured in rat OM and liver microsomes (Mean \pm Standard Deviations). Metabolites were separated by HPLC. Dextrorphan was detected by fluorimetry, with an excitation wavelength of 200 nm and an emission wavelength of 305 nm, and quantified by reference to a standard, 2005 concentration. All others metabolites were quantified after on-line radiochemical detection using reference products. Statistical significance of differences was tested with the Student's *t*-test.

ND: not detectable, n=number of experiments, x: unidentified metabolite, NS: not significant.

substrates	Measured metabolites	Specific Activities (pmol/min/mg of proteins)		Student's <i>t</i> -test (P<)
		OM (n=4)	Liver (n=4)	
phenacetin	acetaminophen	11191 \pm 1923	1431 \pm 29	0.01
chlorzoxazone	6-OH chlorzoxazone	10070 \pm 1722	3210 \pm 415	0.01
tolbutamide	OH tolbutamide	8 \pm 0	115 \pm 17	0.01
lauric acid	ω -OH lauric acid	548 \pm 73	473 \pm 88	NS
dextromethorphan	dextrorphan	2795 \pm 173	2291 \pm 203	0.01
testosterone	2 α OH-testosterone	ND	4500 \pm 837	
	2 β OH-testosterone	2524 \pm 291	ND	
	6 α OH-testosterone	ND	ND	
	6 β OH-testosterone	459 \pm 67	1800 \pm 231	0.01
	7 α OH-testosterone	ND	ND	
	15 α OH-testosterone	3864 \pm 482	ND	
	15 β OH-testosterone	2454 \pm 239	ND	
	16 α OH-testosterone	ND	5560 \pm 1066	
	16 β OH-testosterone	ND	ND	
	androstenedione	608 \pm 42	3600 \pm 1208	0.01
	x	1741 \pm 226	ND	

Table 3

Inhibition of CYP-dependent microsomal activities measured in rat OM by various chemicals. With the exception of diethyldithiocarbamate, each inhibitor was tested at two different concentrations. Only one experiment was performed because of the small amount of available material.

Substrates	Inhibitors	% Inhibition
Testosterone	Ketoconazole 1 μ M	0%
	10 μ M	10%
	5-MOP 10 μ M	38%
	50 μ M	84%
8-MOP 2 μ M	10 μ M	60%
		81%
Phenacetin	Furafylline 3 μ M	50%
	30 μ M	55%
	α -naphthoflavone 0,1 μ M	26%
	5 μ M	94%
5-MOP 10 μ M	50 μ M	95%
		100%
8-MOP 2 μ M	10 μ M	96%
		100%
Chlorzoxazone	Diethyldithiocarbamate 20 μ M	48%
	5-MOP 10 μ M	58%
	50 μ M	89%
	8-MOP 2 μ M	62%
	10 μ M	87%
Dextromethorphan	Quinine 5 μ M	1%
	10 μ M	23%
	5-MOP 10 μ M	79%
	50 μ M	100%
8-MOP 2 μ M	10 μ M	94%
		100%

Table 4

Determination of the apparent kinetic parameters (K_m , V_{max}) and efficiency of the CYP for activities toward four model substrates in rat olfactory mucosa and hepatic microsomes. Activities were calculated from the measurement of the residual substrate concentrations.

Substrates	K_m μM	V_{max} $\mu\text{mol}/\text{min}/\text{mg}$ of microsomal protein	V_{max}/K_m $\text{ml}/\text{min}/\text{mg}$	K_m μM	V_{max} $\mu\text{mol}/\text{min}/\text{mg}$ of microsomal protein	V_{max}/K_m $\text{ml}/\text{min}/\text{mg}$
	olfactory mucosa			liver		
Testosterone	2.95	9.92×10^{-3}	3.36	5.69	16.0×10^{-3}	2.81
Phenacetin	3.04	9.50×10^{-3}	3.12	39.2	2.18×10^{-3}	0.056
Chlorzoxazone	18.7	9.94×10^{-3}	0.53	220	3.91×10^{-3}	0.018
Dextromethorphan	6.11	1.49×10^{-3}	0.24	2.98	1.71×10^{-3}	0.57

Table 5

Metabolic properties of rat CYP recombinant isoforms toward six model substrates: a comparative and semi-quantitative analysis of activities reported in the literature. The isoform with the highest activity toward a given substrate among the 19 CYP isoforms is considered as having the one hundred percent reference activity (i.e.: 40 pmol/min/pmol CYP1A1 for phenacetin; 23 pmol/min/pmol CYP2E1 for chlorzoxazone; 36 pmol/min/pmol CYP4A1 for lauric acid; 3.3 pmol/min/pmol CYP2D2 for dextromethorphan and 9.2 pmol/min/pmol CYP3A1 for testosterone). The percentage of activity of the other isoforms toward the same substrate is calculated pro-rata from this reference activity. For lauric acid and testosterone, both engendering more than one metabolite, the 100% reference activity is chosen as being the highest activity among the CYP isoforms and among all the produced metabolites. (data adapted from Dutton et al., 1987; Waxman et al., 1987; Halvorson et al., 1990; Liu et al., 1996; Nguyen et al., 1999; Rowlands et al., 2000; Wang et al., 2000; Kobayashi et al., 2002; Warrington et al., 2004). No rat recombinant CYP2G1 and CYP4B1 have been developed until now.

model substrates	formed metabolites	CYP recombinant isoforms																		
		1A1	1A2	2A1	2A2	2A3	2B1	2B2	2C6	2C11	2C13	2D1	2D2	2E1	3A1	3A2	3A9	4A1	4A2	4A3
phenacetin	acetaminophen	75-100%	1-24%	NM			NM													
chlorzoxazone	6OH-chlorzoxazone			NM	NM							NM	NM	75-100%						
tolbutamide	OH-tolbutamide																			
lauric acid	ω OH-lauric acid																			
	ω-1 OH-lauric acid																		NM	
dextromethorphan	dextrorphan		NM	NM	NM		NM		NM	NM	NM	NM	75-100%	NM		NM				
testosterone	2αOH-testosterone			NM	NM	NM	NM													
	2βOH-testosterone			NM	NM		NM			NM										
	6αOH-testosterone					NM	NM			NM										
	6βOH-testosterone	1-24%		NM		NM	NM													
	11αOH-testosterone					NM	NM													
	15αOH-testosterone			NM				NM			NM									
	15βOH-testosterone			NM	NM		NM				NM									
	16αOH-testosterone			NM	NM		NM													
	16βOH-testosterone	NM		NM	NM		NM				NM									
androstenedione	NM		NM		NM															

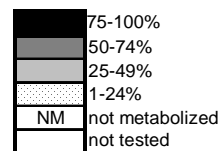


Table 6

Inhibition of rat CYP recombinant isoforms: a comparative and semi-quantitative analysis of the inhibitions reported in the literature. This Table presents, for each inhibitor, the percentage of inhibition toward each of the 19 CYP isoforms, as reported in the literature. (data adapted from Liu et al., 1996; Koenigs et al., 1998; Kobayashi et al., 2003).

inhibitors	CYP recombinant isoforms																			
	1A1	1A2	2A1	2A2	2A3	2B1	2B2	2C6	2C11	2C13	2D1	2D2	2E1	3A1	3A2	3A9	4A1	4A2	4A3	
ketoconazole		50-74%	1-24%					75-100%	1-24%			1-24%	NI	50-74%	75-100%					
furafylline		75-100%	25-49%					75-100%	50-74%			NI	NI	1-24%	1-24%					
α -naphthoflavone																				
diethylthiocarbamate																				
quinine								25-49%	25-49%			75-100%								
methoxsalen		75-100%	75-100%		75-100%	50-74%		75-100%	75-100%			NI	25-49%	1-24%	50-74%					

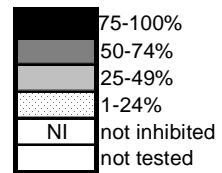


Figure 1

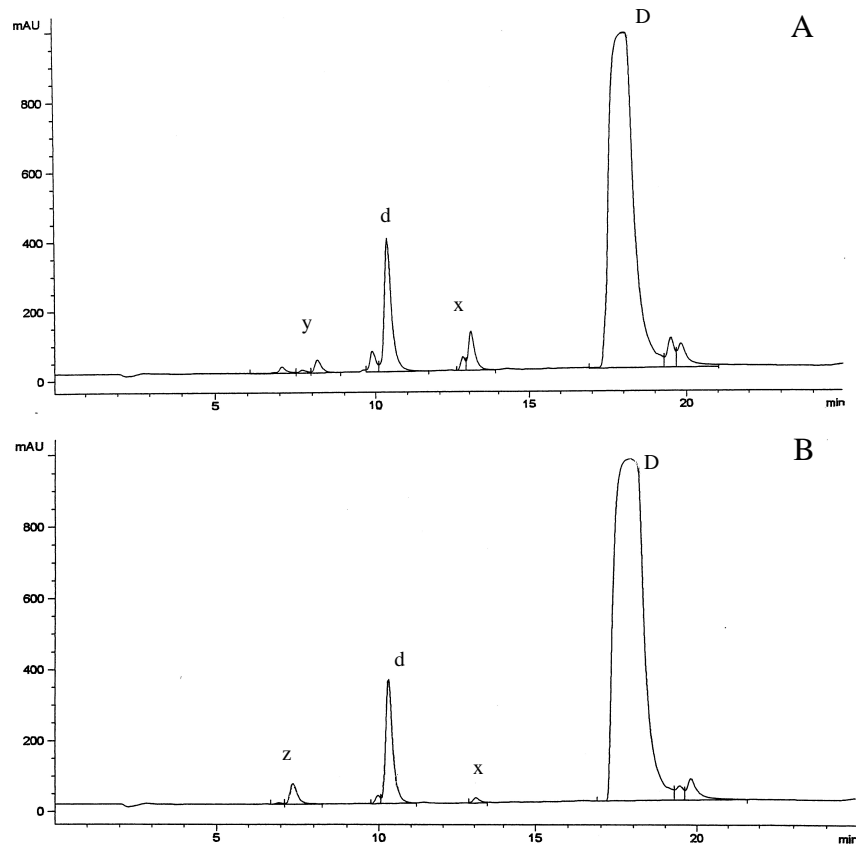


Figure 2

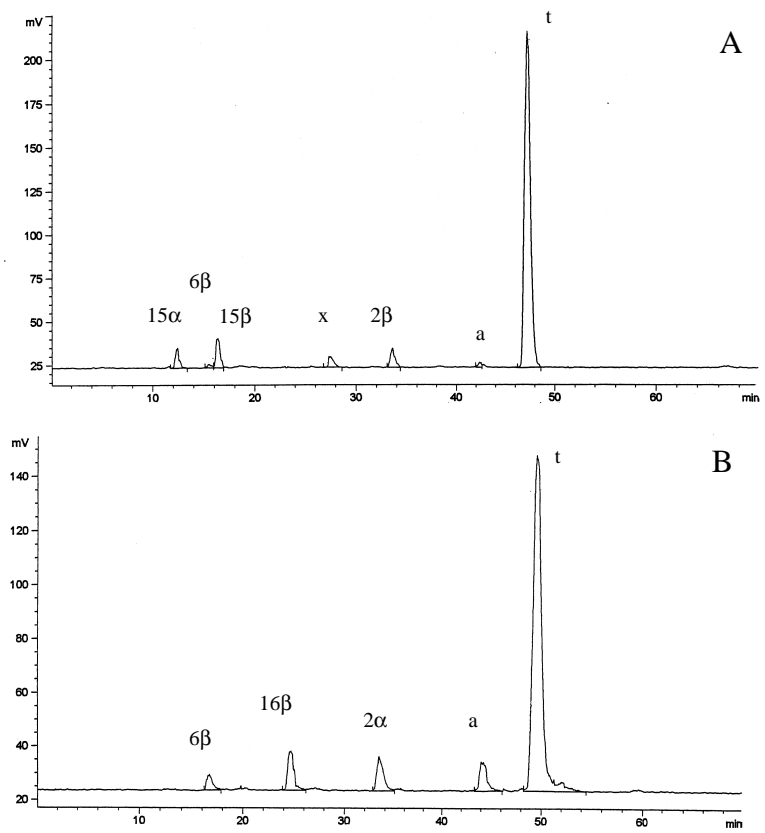


Figure 3

